Check for updates

Compartmentalised single-chain nanoparticles and their function

Justus F. Thümmler [ID] and Wolfgang H. Binder [ID] *

Single-chain nanoparticles (SCNPs) are generated by intramolecular collapse and crosslinking of single polymer chains, thus conceptually resembling the structures of folded proteins. Their chemical flexibility and ability to form compartmentalised nanostructures sized ~1 nm make them perfect candidates for numerous applications, such as in catalysis and drug delivery. In this review we discuss principles for the design, synthesis and analysis of SCNPs, with a focus on their compartmentalised structures, highlighting our own previous work. As such compartments offer the potential to generate a specific nanoenvironment *e.g.* for the covalent and non-covalent encapsulation of catalysts or drugs, they represent a novel, exciting, and expanding research area. Starting from the architectural and chemical design of the starting copolymers by controlling their amphiphilic profile, the embedding of blocks-, or secondary-structure-mimetic arrangements, we discuss design principles to form internal compartments inside the SCNPs. While the generation of compartments inside SCNPs is straightforward, their analysis is still challenging and often demands special techniques. We finally discuss applications of SCNPs, also linked to the compartment formation, predicting a bright future for these special nanoobjects.

1. Introduction

When components in a chemical or biological system require a specific localised environment, Nature has developed sophisticated separation entities on different length scales to spatially and temporally separate processes.[1] Thus compartmentalisation is present in, *e.g.* each cellular compartment, like cell-membranes or organelles (mitochondria,[2] cell-nuclei[3]); in viral capsids segregating and protecting the embedded nucleic-acids from the environment and mediating specific entry into cells;[4] and most importantly in chemical reaction "organelles", separating reactants in a chemical reaction and further allowing separation of the reactants after workup. Especially compartments on the nanoscale (below 100 nm) have emerged as a fundamental principle to direct

Institute of Chemistry, Faculty of Natural Science II, Martin Luther University Halle-Wittenberg, von-Danckelmann-Platz 4, D-06120, Halle (Saale), Germany. E-mail: wolfgang.binder@chemie.uni-halle.de

Justus F. Thümmler studied chemistry at the Martin-Luther-University in Halle. After his specialization in physical chemistry of polymers and his master thesis at the Fraunhofer IMWS, he worked on his PhD thesis on near-infrared fluorescent single-chain nanoparticles and their nanostructural and photophysical characterization in the group of Professor Wolfgang H. Binder which he finished in 2024. In the Binder group he is currently working as researcher, continuing his work on single-chain nanoparticles.

Justus F. Thümmler

Wolfgang H. Binder is currently a full professor of macromolecular chemistry at MLU since 2007. Born in Vienna, Austria (1969), he studied chemistry at the University of Vienna, obtaining his PhD in organic chemistry in 1995, followed by postdoctoral stays (1995–1997) with Prof. F. M. Menger (Emory University, Atlanta, GA) and Prof. J. Mulzer (University of Vienna), then completing his habilitation (2004), subsequently as associate professor from 2004 to 2007. His research interests are directed toward polymer synthesis, supramolecular chemistry, self-healing polymers, artificial membranes, and nanotechnology.

Wolfgang H. Binder

chemical and biological reaction pathways, such as in enzymes in their hydrophobic/hydrophilic pockets[5] allowing the specific positioning of reactants towards catalytic sites,[6] or in (biomimetic) catalysis, then generating a specific reaction environment. Such compartments can be selective in hosting a specific sort of molecules in pockets, clefts, or porous structures, where a specific reactivity can be reached, given that dynamic processes are embedded to allow adaption and release of products. Organic (nano)particles like micelles, liposomes, lipid nanodiscs or proteins use organic molecules as building blocks often *via* self-assembly into higher organized systems. In the last decades many such compartmentalised systems have been developed, such as block-copolymer-assemblies,[7] dendrimers,[8] or nanogels,[9] forming compartments in the nanometre range (*e.g.* biomembranes,[10] micelles,[11] dendritic boxes[12]) up to the micron range (such as liposomes[13] or emulsion droplets[14]).

Single-chain nanoparticles (SCNPs) have recently emerged as a special class of nanosystems displaying sizes in the range of 5–20 nm, depending on the polymer chain they are formed from.[15] Based on their size, the chemical versatility of their generation and the multifaceted embedding of functional entities during their synthesis, they have been proven to be most versatile and adaptable in view of catalysis,[16] drug delivery,[17] or as enzyme-mimetics.[18] SCNPs are crosslinked polymeric nanostructures that are formed from intramolecularly collapsed

single polymer chains in a process reminiscent of protein folding.[18] Conceptually, they are a special, extremely small type of nanogel, but due to their unique architecture, versatility of synthesis and the final properties they create a completely new class of polymeric nanoparticles.

It recently was discovered that even those small-sized SCNPs can display an internal structure equipping them with specialised functions beyond a pure encapsulation (see Fig. 1),[19] usually significantly smaller than the already small particles themselves. The formation of these compartments inside those SCNPs is driven by molecular assembly (supramolecular/liquid crystalline assembly);[20] polymer/polymer phase segregation;[19b,19c] or by amphiphilic segregation based on solvent/polymer segregation so finally guided by a sequential folding process.[21] They are comparable to pockets normally found in, *e.g.* enzymes, where highly specialised reaction environments are generated to spatiotemporally catalyse specific reactions.

They can be fundamental to tune optical effects with embedded dyes,[24] induce special photothermal swelling effects[19e,19f] and conformational changes by photophysical crowding effects.[25]

Since Pomposo *et al.* have reviewed on internally and externally confined SCNPs in 2020,[15a] the development of confined/compartmentalised SCNPs has become a major interest among polymer researchers. It is in this article that we describe the latest developments in the generation of such structures also based on own
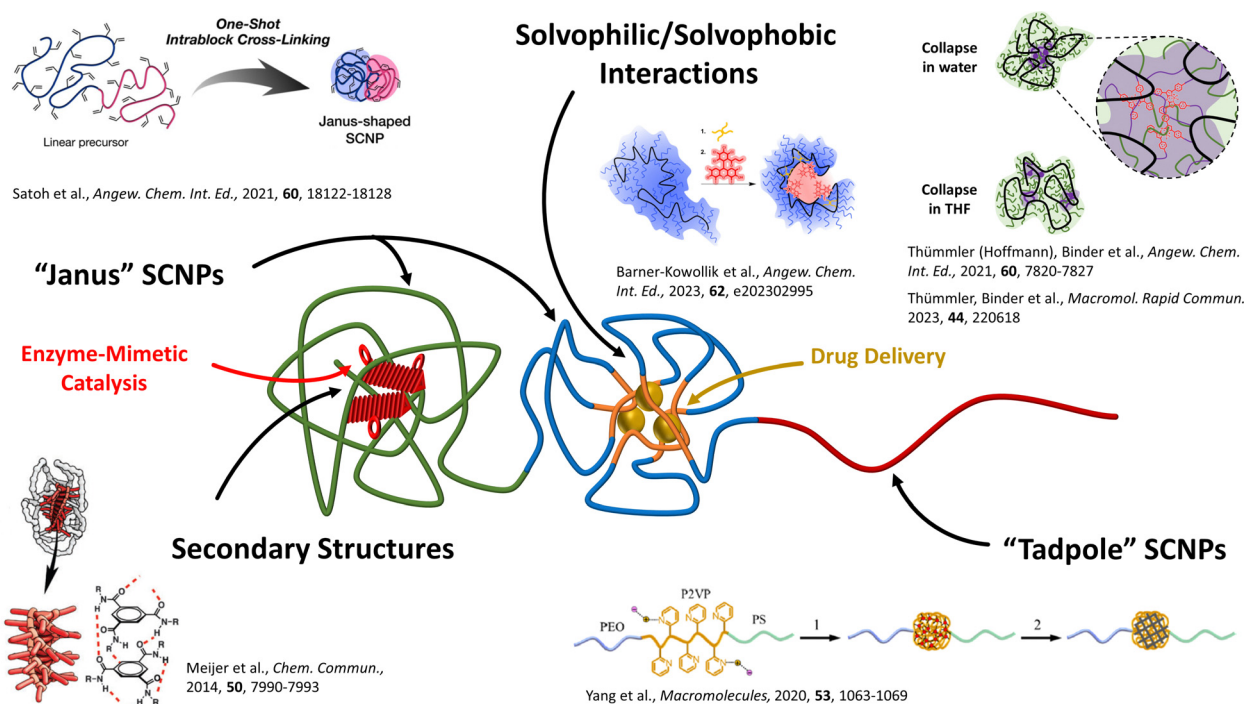

Fig. 1 Illustration of compartmentalised structures in single-chain nanoparticles (SCNPs) and their applications in enzyme-mimetic catalysis and drug delivery. Block-copolymers can be collapsed into Janus-SCNPs by crosslinking the respective individual block. One or more non-functionalised blocks can create tadpole-shaped SCNPs, which structurally resemble surfactants or lipids. Secondary-structure-like compartments can be achieved, *e.g. via* H-bonding BTA-stacks. Solvophilic/solvophobic interactions are the main driving force of compartmentalised structures, since the solvophobic parts of the precursor polymer can phase-segregate, resulting in a core−shell structure. Reproduced with permission from: Wiley VCH, copyright © 2021,[19b] 2023 (open access CC BY-NC 4.0);[19a,19e] the Royal Society of Chemistry, copyright © 2014 (open access CC BY 3.0);[22] and the American Chemical Society, copyright © 2020.[23]

contributions during the past years, with a focus on principles, analytical methods, as well as applications wherein the compartments are exploited. We focus on the principles guiding SCNP formation, together with the physicochemical effects guiding the formation of the internal compartments inside the SCNPs. With this perspective we take our starting point at previously published papers on SCNPs, moving beyond the chemical and physical principles described therein.

2. Design of compartmentalised single-chain nanoparticles (SCNPs)

Similar to proteins, which are formed by collapse of a single peptide-chain, SCNPs are generated by single-chain collapse at high dilutions dominated by solvent-assisted intramolecular *vs.* intermolecular-assembly (Fig. 2).[26] Subsequent internal cross-linking interactions, *e.g. via* H-bonds, click-reactions, or metal complexation, can preserve the collapsed chains in these conformations.[27] Experimentally, single-chain collapse is conducted at high dilutions ($<10^{-5}$–10^{-6} M).[26] The internal cross-linking interactions then preserve the collapsed chains in the so reached conformations.[27]

Critical aspects to control formation of compartments inside the SCNPs are therefore (a) the design of the polymer that is folded into a SCNP, controlling its shape, internal structure, solubility, biocompatibility, or stimuli-responsive behaviour; (b) the conditions of chain-collapse (such as solvens and temperature), and the subsequent crosslinking methods to "freeze-in" the previously generated structures. As the processes involved during SCNP formation are comparable to the folding of peptides into secondary structures with the additional quest to prevent a subsequent aggregation of the folded macromolecules, the final shape of the SCNP as well as the internal compartments and functionality are strongly influenced by the architecture of the individual polymer chains, the solvent that is used during the collapse reaction, and the solvent/monomer-interactions of the individual monomer units during chain-collapse and -crosslinking. It is evident that, *e.g.* random copolymers without specific solvent/monomer
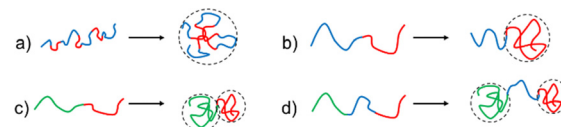

Fig. 3 Examples of compartment-formation achieved by different types of copolymers, leading to single-chain nanoparticles. (a) A random copolymer collapsing into a globular or random shaped SCNP; block copolymers collapsing into (b) a tadpole-shaped SCNP, (c) a Janus SCNP, and (d) a dumbbell-shaped SCNP. Blue: non-crosslinking polymer segments. Red and green: potentially crosslinking polymer segments.

interactions are expected to result in more random, sparse structures in the final SCNP, whereas the use of sequential, diblock-/triblock- or sequence-specific copolymers, can easily yield compartmentalised SCNPs, as shown in Fig. 3.[28]

Control over the copolymers' architecture during synthesis is crucial to reach the desired SCNP with a specific compartmentalised structure. Often living polymerisation techniques are used to this purpose, such as controlled radical polymerisations like atom transfer radical polymerisation (ATRP),[29] nitroxide mediated polymerisation (NMP),[30] reversible-addition–fragmentation chain-transfer (RAFT) polymerization,[24,31] or Ru-catalysed living radical polymerisation;[32] as well as other methods like living anionic and cationic polymerisation,[19c,33] group transfer polymerisation (GTP)[34] or ring opening metathesis polymerisation (ROMP).[35] Together with the placement of the individual monomers, these polymerisation techniques reach low polydispersities and high molecular weights (>20 kDa up to 100 kDa or more), all resulting in precisely engineered sizes (5–20 nm) and chemical compositions of the SCNPS. Bioinspired SCNPs are especially attractive for biomedical application because of their biocompatibility when embedding polypeptides and carbohydrates as backbone materials, optionally generated by biosynthesis,[36] which can further be modified then deviating from their natural composition and structure to yield highly functional SCNPs.[37] Polypeptides can also be produced synthetically, by performing ring opening polymerisations of *N*-carboxyanhydrides.[38]

2.1. Collapsing methods

The condition upon single-chain collapse can engineer a chemical functionality inside/around the SCNP to form different types of particles from one and the same polymer chain. In this chapter we are highlighting some basic principles of the analysis and formation of SCNPs.

Firstly, preventing intermolecular crosslinking and aggregation is central and must be ensured during the collapse and crosslink procedure of SCNPs, since only then the intramolecular interactions will result in (stable & useful) single-chain nanoparticles. To this end, various methods have been developed, all having in common that they require high dilutions in the range of <1 mg mL^{-1} for polymers, equal to $\sim 10^{-6}$ M for reactive groups along the polymer chains.[26,39]

Generating SCNPs on a reasonable scale with high reproducibility requires (a) fast and efficient reactions under high dilutions and (b) defined experimental conditions during
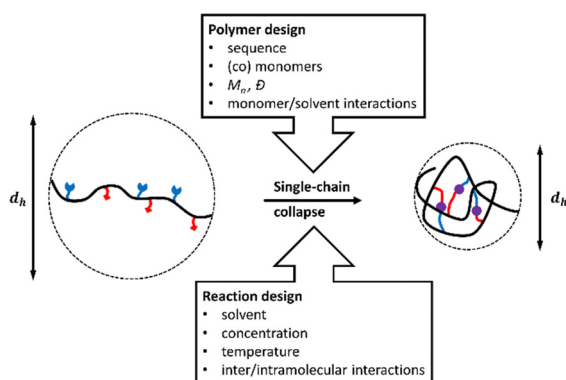

Fig. 2 Factors influencing the structure of compartimentalized single-chain nanoparticles (SCNPs) by collapse of a single polymer chain, often with a reduction of the hydrodynamic diameter d_h.
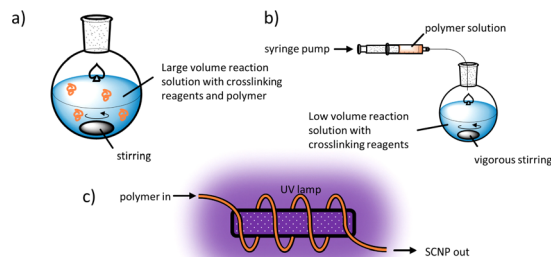
Fig. 4 Illustration of experimental procedures for the synthesis of SCNPs using (a) a large volume reaction solution with a low concentration of polymer, (b) the continuous-addition protocol, and (c) a photochemical flow reactor.

single-chain collapse. Often SCNP syntheses are conducted using a continuous-addition protocol as developed by Harth et al.,[17,30a,39b,40] where a concentrated polymer solution is slowly dropped into a solution with the reactants under vigorous stirring, see Fig. 4b. The droplet entering the reaction solution thus should react efficiently resulting in intramolecular crosslinks only. Since all reactive groups along the polymer chains of this droplet are so completely consumed, the reactive groups of the next droplet will again react only intramolecularly under these diluted conditions allowing syntheses under much higher final concentrations and yields in the gram-scale.[41]

Upscaling of SCNP-synthesis is possible with flow reactors, wherein the reaction is taking place along a tube through which a solution is flowing, addressing larger scale syntheses. As reported by Barner-Kowollik and Diesendruck et al.,[42] a polymer that contains photodimerizing groups can flow through a tube that is wrapped around an ultraviolet (UV) lamp, as depicted in Fig. 4c, to effect photo crosslinking after single-chain collapse. This way SCNPs can be synthesised with shorter irradiation times and higher conversions than in a comparable reaction in a batch reactor, making this method quite efficient.

2.2. Crosslinking methodologies to stabilise formed SCNPs and their compartments

The crosslinking strategies used to stabilize the initially collapsed SCNP into the final, irreversible structure are crucial in maintaining the initially, collapsed polymer conformation. Both, covalent and non-covalent crosslinks can be applied. In addition, dynamic crosslinks, usually supramolecular or dynamic covalent bonds, allow for an additional responsive element inside the SCNPs, potentially allowing a later chain reorganization or "error" corrections of eventually misfolded compartments.

Thus supramolecular interactions such as hydrogen bonds are effective to form SCNPs, using ureidopyrimidinone[29a,35a,43] or Hamilton wedges with cyanuric acid derivatives.[44] Chiral benzene-1,3,5-tricarboxamides (BTA) have emerged as a non-covalent crosslinking method that do not only provides hydrogen bonds as linking units, but embeds a chiral compartment inside the SCNP core, similar to α-helices in proteins.[20b,22,29d,35d,45] β-Hairpin-like single-chain structures can be formed using supramolecular quadrupole π-stacking interactions between electron-rich benzene moieties and electron deficient pentafluorobenzene moieties in an ABC-block copolymer with a polystyrene, and a polypentafluorostyrene block, separated by a spacer block.[46] Other supramolecular interactions, such as metal complexes can be used for the crosslinking of a single polymer chain with the ligands covalently bound to the polymer chain, thereby utilising the complexation of a metal ion.[23,35f,47] This interaction can also be used to incorporate a metal catalyst inside the SCNP to synthesize an enzyme analogue.[35e,35f,47f,47g,48]

Less dynamic but more direct is the use of covalent crosslinks, which fix the internal nanostructures even if external properties like solvent quality are changed. Besides simple organic reactions, like nucleophilic substitutions,[30c] ester/amide formations,[21b,25,36b,37b,49] or polymerisations of vinyl groups[33,50] and cyclic esters,[51] "click" reactions[52] have been proven useful due to their high efficiency under mild (even aqueous) reaction conditions. The copper catalysed azide–alkyne click reaction (CuAAC) became one of the most important methods used by us for covalently crosslinking SCNPs, based on its large free reaction enthalpies (>50 kJ mol^{-1}), resulting in high yields, and the insensitivity to many other functional groups and solvents used therein.[53] We[19d–g,52,54] and others[40,55] have used the CuAAC extensively to stabilize the collapsed polymers and transform them into the final SCNPs under mild conditions. The wide variety of possible covalent reactions then allows the subsequent incorporation of functionalities even after the completed single-chain collapse reaction, like the incorporation of a specific number of dye molecules,[19e] or the embedding of responsivities to external stimuli[19f] to change the structure of the SCNPs. This further allows synthesis of covalently crosslinked SCNPs that can be dynamically opened and closed by photothermal-effects, transferring energy to the outside of the SCNP-shell.[56] Further mild crosslinking chemistries are photodimerizations[29c,35g,42a,57] and disulfide bridges[35c,58] reaching dynamic covalent SCNPs that are especially interesting for biomedical applications since their responsivities can increase their drug delivery efficiency and biodegradability.[50]

3. Compartmentalised SCNPs

To generate compartments located at the outside of an SCNP block copolymers can be used. Depending on the type, order, and functionality of the respective blocks differently shaped SCNP systems can be achieved, resulting in phase segregating properties of the different parts of the SCNPs. Examples for compartmentalised SCNPs are shown in Fig. 1, including their chemical properties, collapse methodologies, and special features. As depicted in Fig. 3b, collapsing a block copolymer with one non-reactive, solvophilic block and s solvophobic and reactive block, tadpole-shaped SCNPs can be synthesised[19c] resembling the structure of surfactants. Because of their exposed blocks such SCNPs can further aggregate into micelle- or vesicle-like superparticles via their exposed blocks, relying on Flory–Huggins principles.[29c,59] Block copolymers with two reactive blocks can collapse into two-sided "Janus" SCNPs

(see Fig. 3c).[35h,57i] Satoh *et al.* showed that also blocks with the same crosslinking functionality will collapse into Janus SCNPs because of the higher reactivity of proximal sites.[19b] Adding a non-reactive spacer block in between the crosslinkable blocks then generates dumbbell-shaped SCNPs as depicted in Fig. 3d.[49a,60]

Forming compartments in the inner core of the SCNPs usually starts with the formation of "unimolecular micelles", similar to single-chain nanoparticles, but formed without subsequent crosslinking chemistry. They can form core–shell-like structures in water with hydrophilic sidechains in the shell and hydrophobic sidechains in the core, as depicted in Fig. 5a. Their hydrophilicity in the shell can be achieved by using poly ethylene glycol (PEG)[32,61] or ionic sidegroups.[62] The core-building, hydrophobic sidechains can be introduced by using either aliphatic[32,61c,62] or fluorinated sidechains,[61a,61b] which in turn forms compartments by hydrophilic/hydrophobic solvent interactions. Those assemblies have been used as antimicrobial compounds[61c] and are interesting as drug delivery systems, covalently binding or encapsulating drugs inside their hydrophobic core,[62] as controlled drug-release systems, similar to classical micellar structures (Table 1).[61a]

The synthesis of crosslinked, compartmentalised SCNPs is based on the same mechanism as the formation of unimolecular micelles but with an additional crosslinking reaction to retain the compartmentalised structure even after concentration or solvent changes. As depicted in Fig. 5b, the different interacting individual segments can lead to the formation of core–shell structured SCNPs. Ideally, the crosslinking moieties are solvophobic so that the inner core of the SCNP is stabilised, with the crosslinking reactions now taking place only in the core, resulting in stronger compartmentalised structures.[35d,35g,67]

As mentioned above the solvents in which the collapse and crosslinking reactions take place have a major influence on the internal compartmentalised structures of the SCNP. A solvent or solvent mixture that shows good quality for all segments of the precursor polymer, including the crosslinking units, will result in non-controlled, sparse SCNPs,[35d,35g] while a solvent with a poor quality for all segments can result in multi-chain aggregation instead of the collapse of single chains.[35g] Exemplary, Simon *et al.* showed that the single-chain collapse of a comb-copolymer with poly-isobutylene (PIB) sidechains (M_n = 3.5 kDa) and anthracene crosslinking units resulted in different compartmentations inside the formed particles, depending on the solvent quality.[35g] The photodimerization of the anthracene units in pure tetrahydrofuran (THF), a good solvent for both monomer units, resulted in low conversions and sparse SCNPs, while the same reaction in pure hexane, which is only a good solvent for the PIB units, resulted in multi-chain particles. Only a mixture of both solvents was able to yield high conversions and well-defined core–shell structured SCNPs.

We[19e] used amphiphilic polymers to prepare core–shell structured SCNPs, reaching different compartments depending on the solvent and crosslinker used during single-chain collapse. The precursor polymer, a random copolymer with hydrophilic PEGMA monomers and hydrophobic azide-functionalised monomers, allows crosslinks *via* CuAAC in mixture with hydrophobic, bivalent alkynes with and without functionality (radical TEMPO label, fluorescent aBOD-label, octadiyne) for a subsequent analysis of the SCNPs (see Fig. 6).

Chain collapse was performed by CuAAC in water and THF as selective and non-selective solvent, respectively. It was hypothesised that the reaction in water would lead to core–shell structured SCNPs because of the amphiphilic nature of the precursor polymer and the hydrophobicity of the crosslinkers, while the same reaction in THF, a solvent which is almost equally well solubilizes all monomers of the polymer and crosslinkers, would lead to SCNPs without defined internal structures.

Extensive analyses *via* CW-EPR and time resolved fluorescence spectroscopy revealed that the internal structure is strongly guided by the polarity of the solvent, resulting in formation of dense hydrophobic cores, when the collapse reactions are performed in water. Using solely the labelled crosslinkers the formation of a core–shell structure was reduced, whereas mixtures of the rigid label-crosslinkers with the flexible octadiyne resulted in the desired core–shell structures as depicted in Fig. 7.

The relation between the flexibility and length of a crosslinker and the resulting nanostructure of the SCNP is known in literature,[68] caused by the formation of long range interactions for longer and more flexible crosslinkers, resulting in more compact and dense SCNPs directly linked to the desired applications of SCNPs. We embedded fluorescent dyes for pump–probe photoacoustic (PA) imaging as crosslinkers, so exponentially increasing PA signals, while the unstructured SCNPs showed only weak and non-exponential PA signals.

We further tuned the hydrophobicity of the SCNP core by changing the fraction of hydrophobic units in a similarly designed SCNP system (see Fig. 8) to reach a closer mimicry of proteins and enzymes, modifying with (i) purely hydrophobic, aliphatic sidechains and (ii) hydrophobic, fluorinated sidechains.[54]

By tuning the composition of the copolymer (variation of the hydrophobic (aliphatic/fluorinated) and hydrophilic monomers) not only core–shell structured SCNPs but different compartments were formed inside the aliphatic and fluorinated cores. Solvochromic dyes were added as probes, hydrophobicity-selective *via* an aliphatic or a fluorinated sidechain, proving by time resolved fluorescence spectroscopy a stronger affinity of the fluorinated
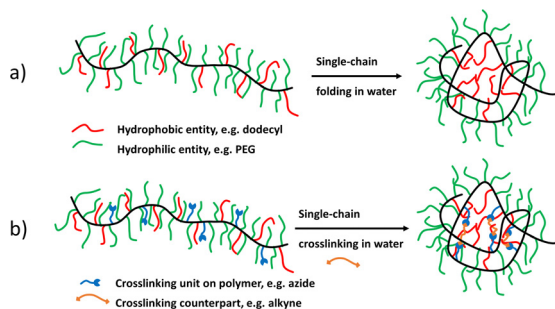

Fig. 5 (a) An amphiphilic random copolymer folding into a unimolecular micelle in water. (b) An amphiphilic random copolymer with crosslinking units collapsing and crosslinking into a single-chain nanoparticle.

Table 1 Examples for compartmentalised SCNPs published since 2020, including their chemical structure, collapse methodologies, and special features/applications. Different colours indicate different compartments inside the SCNP
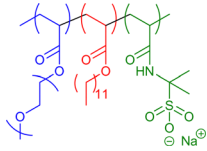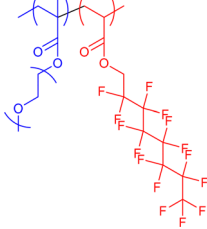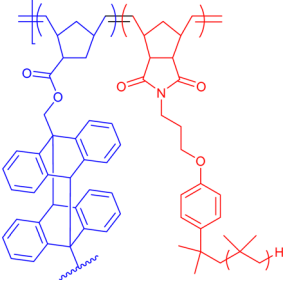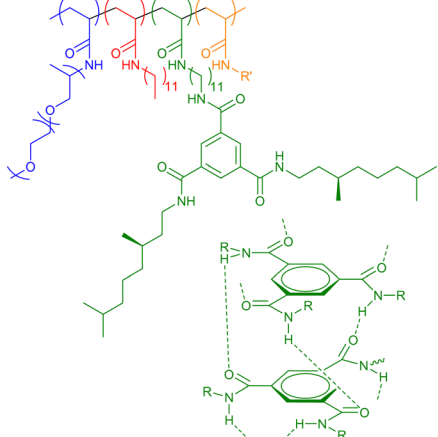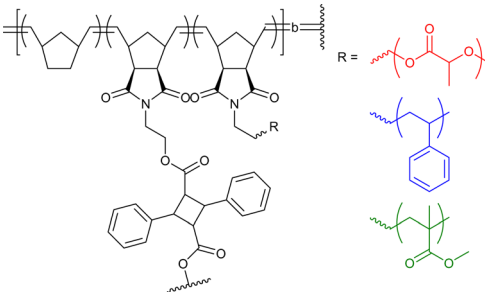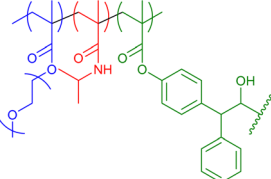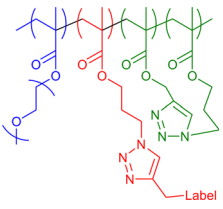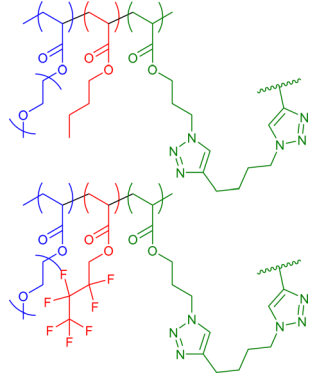
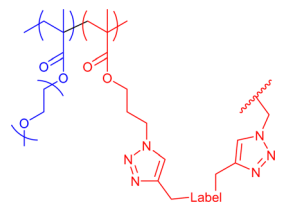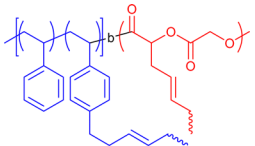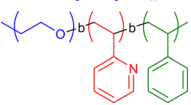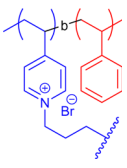| Chemical Structure	M_n/kDa	Collapse Methodology	D_h/nm	Special Features/Applications	Ref.
	10–40	Hydrophilic–hydrophobic interactions in water (unimolecular micelles)	12–15	Two hydrophilic units, single-fluorophore encapsulation *via* endgroup functionalisation	62
	13–44	Hydrophilic–hydrophobic interactions in water (unimolecular micelles)	5–8	Encapsulation of drug cargos, thermoresponsive behaviour, invertible micelle upon solvent exchange to hexafluorobenzene	61a,61b,63
	320–460	Anthracene photodimerization in THF/hexane mixtures	10	Core–shell structure formation in non-aqueous system	35g
	8–93	Chiral H-bonding of BTA in water	10–14	Helical structure in SCNP core, incorporation of dyes, catalysts, and other functionalities (R' in structure)	45e,45f,64
	300–430	Cinnamic acid photodimerization in THF	6.6	Differently miscible blocks, block-order-dependent nanostructure	35h
	18–29	Benzophenone photo-crosslink in water at different temperatures	12–16	SCNP size dependent on crosslinking temperature, thermoresponsive swelling-deswelling of core	65

Table 1 (continued)

Chemical Structure	M_n/kDa	Collapse Methodology	D_h/nm	Special Features/Applications	Ref.
	36–44	Internal CuAAC in water	5–10	Covalent encapsulation of multiple fluorescent and radical labels, thermoresponsive swelling-deswelling of core	19f,19g
	13–19	CuAAC in water with external bivalent crosslinker	6–12	Differently hydrophobic environments for either aliphatic or fluorinated SCNP core, specific encapsulation of aliphatic/fluorinated cargos	54
	35	CuAAC in water or THF with external bivalent and functional crosslinker	6–12	Internal structure dependent on solvent medium and crosslinker bulkiness, covalent encapsulation of multiple crosslinking fluorescent and radical labels	19e
	20–23	Intrablock crosslinking via olefin methathesis in DCM	6–8	Janus-shaped SCNP, one-shot crosslinking of spatially close reactive sites, lamellar phase separation	19b
	n.a.	Co complexation in o-dichlorobenzene	12	Tadpole structure with two tails, magnetic and catalytically active cobalt generation upon thermolysis	23
	475	Amine quaternisation in DMF	34	Tadpole SCNP, head can actively graft on inert surfaces	66

dye to the fluorinated core. Similar, an aliphatic EPR label was found to preferably enter the aliphatic core compared to the fluorophilic core. Hence, the different types of cores effected their affinity to bind external hydrophobic probes, mimicking the selectivity of enzymatic structures.

Response of the compartment formation to temperature can be reached via thermoresponsive segments in the precursor polymer chain, e.g. poly(oligo ethylene glycol) methacrylates (PEGMA) or poly N-isopropyl acrylamides (PNIPAM). These polymers show lower critical solution temperature (LCST) behavior in water, becoming insoluble in water above the cloud point temperature T_{cp}. As demonstrated by Lu et al.,[65] at temperatures well below T_{cp} of those segments, the SCNP synthesis will result in sparse non-compartmentalised SCNPs,

whereas at temperatures above T_{cp}, core–shell structured SCNPs with a dense core will be obtained as depicted in Fig. 9. Conducting the SCNP synthesis at medium temperatures, a core–shell structure is generated, but in a less dense state. Swelling of the core with water leads to a thermoresponsivity of the core itself.

Using CW-EPR[19d] and time resolved fluorescence spectroscopy[19f] we demonstrated that the cloud point temperature of the outer shell of the SCNPs can differ from the that of the internal compartments, which leads to contraction of the SCNP system at increased temperatures, still below the macroscopically observed T_{cp}. As SCNPs are monomolecular confined nanogels, they swell with the dispersing solvent.[69] Due to the higher hydrophobicity inside the core of the structured SCNPs compared to their outer shells, the core shows lower and less defined
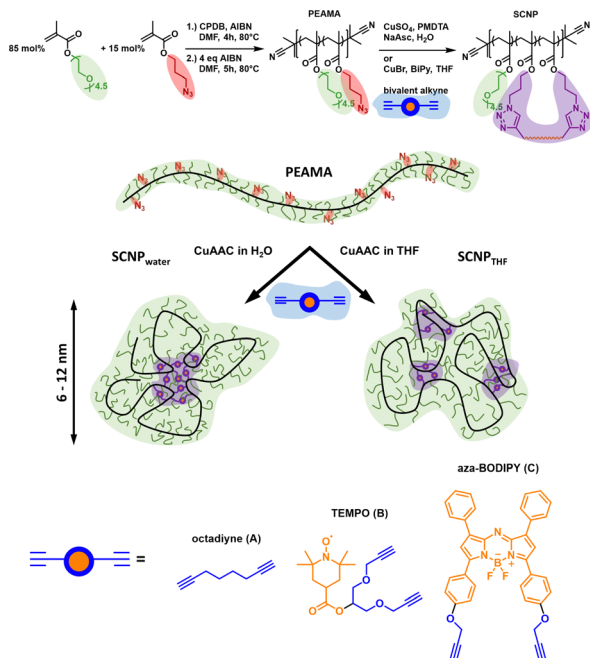
Fig. 6 Concept to create differently structured SCNPs by adjusting the interactions of comonomers during solvent-induced collapse. Reproduced with permission from Wiley VCH, copyright © 2023 (open access CC BY-NC-ND 4.0).[19e]
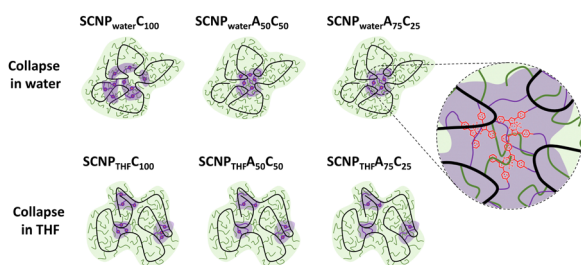

Fig. 7 Schematic illustration of the collapse-solvent and crosslinker-composition-dependence of the internal nanostructure of amphiphilic SCNPs (green: hydrophilic regions, violet: hydrophobic regions). Only those SCNPs formed a core–shell structure which were crosslinked in water with flexible crosslinkers. Reproduced with permission from Wiley VCH, copyright © 2023 (open access CC BY-NC-ND 4.0).[19e]
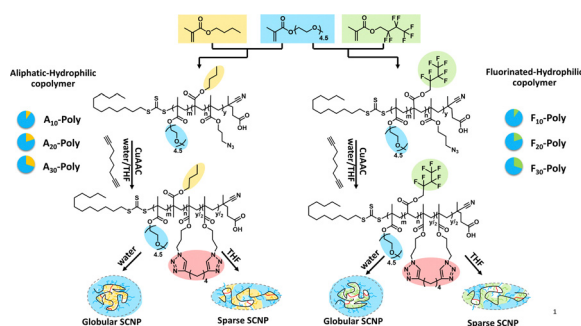

Fig. 8 Synthesis of random copolymers from different methacrylate monomers, displaying different monomer/solvent interactions. Crosslinking after single-chain collapse generates single-chain nanoparticles with different compartments. Reproduced and adapted with permission from the Royal Society of Chemistry, copyright © 2024 (open access CC BY 3.0).
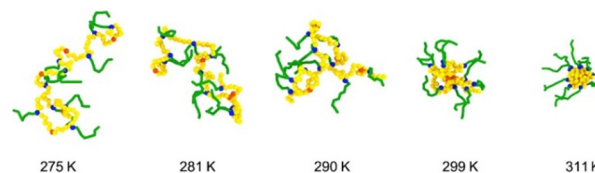

Fig. 9 Simulated chain conformations of a thermoresponsive precursor polymer chain at the indicated temperatures, resulting in so structured SCNPs upon single-chain crosslinking. This figure has been published in CCS Chemistry (2020, open access); "Controlling the Chain Folding for the Synthesis of Single-Chain Polymer Nanoparticles Using Thermoresponsive Polymers" is available under DOI: https://doi.org/10.31635/ccschem.020.202000190.[65]

cloud point temperatures, in turn leading to deswelling of the cores by increasing the temperature, still keeping the SCNPs dispersed. This leads to the previously mentioned contraction of the SCNPs and decreases of d_h, as followed by increased of diffusions, *e.g.* by DOSY-NMR spectroscopy, as well as decreased rotation correlation times in CW-EPR-spectra. Polarity and density changes inside the SCNP cores which follow this contraction play an important role in PA imaging, wherein absorbed NIR light generates heat by pulsed laser excitations of fluorescent dyes. Each laser pulse then changes the core of the SCNP, as depicted in Fig. 10, in turn modulating the photophysical properties of the fluorescent dye, resulting in fluctuating signals. So far, this behavior, an interesting contrast mechanism for PA imaging, has only been observed in our SCNPs, caused by the SCNPs' internal nanostructure.

Compactions of SCNPs as described rely on different thermo-responsivity of core and shell of the SCNPs. A different approach to switch between compacted and expanded SCNPs was followed by Barner-Kowollik *et al.* by introducing *cis/trans*-switchable azo-dyes as crosslinkers.[25] Those dyes are known to reversibly switch between their *cis*- and *trans*-conformation by irradiating with different wavelengths of light. By irradiation with 620 nm light, compactions of the SCNPs were observed by forcing the azo-dye into the *cis*-conformation, while subsequent irradiation with 415 nm light switched the dyes back into the *trans*-conformation, in turn expanding the SCNPs.

Other principles to generate segregated regions inside SCNPs are liquid crystals,[45f,64a] *e.g.* by introducing stilbenes or azobenzenes as side chains to the precursor polymer, resulting in compartmentalised SCNPs upon crosslinking. Inside the relatively unordered SCNPs, those groups will still be able to self-assemble and form (now dynamic) ordered structures which segregate from the polymer backbone.[57f,59c] Thus supramolecular motifs generate internal compartments inside SCNPs *via* the benzene-1,3,5-tricarboxamide
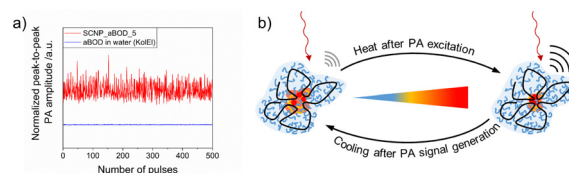

Fig. 10 (a) Fluctuating PA signal of the thermoresponsive SCNPs. (b) Schematic interpretation of the thermoresponsive behavior. Reproduced and adapted with permission from the Royal Society of Chemistry, copyright © 2023.[19f]

(BTA) group introduced by Meijer and Palmans.[45f,64a] BTA molecules form supramolecular assemblies that build helical stacks with threefold intermolecular hydrogen bonds, resembling α-helices of proteins. When BTA molecules are part of a precursor polymer that is dissolved in water, they will self-assemble inside the SCNP's interior, forming intramolecular crosslinks of the polymer chain, segregated from other parts of the polymer to modulate the overall shape of the resulting SCNP.[20b,22,29d,35d,45a,70] These helical stacked structures can be used as platforms for catalytic sites, enabling enzyme-like internal structures which significantly increases catalytic activities.[45b–d,71]

Stepwise folding of individual chains segments of a precursor polymer is the main approach to reach externally compartmentalised SCNPs, like Janus- or dumbbell-shaped SCNPs from block-copolymers after single-chain collapse and crosslink, as described above.[31b,43c,49a,57i] This process tunes the nanostructure and shape of SCNPs originating from random copolymers, e.g. by first preorganising a precursor chain into single-chain ring structure via a hetero Diels–Alder reaction of the end-groups, and then crosslinking the main chain reactive groups via click-chemistry, as shown by Pomposo et al.[55f] This process resulted in significantly stronger compacted SCNPs, compared to the SCNPs, which were obtained by the conventional, non-preorganised, precursor polymer.

4. Characterization of SCNPs and their internal compartments

The characterization of the internal compartmentalisation of SCNPs is challenging due to the usually rather non-defined nature of the SCNPs interior, the inherent dynamics of the SCNP, and polydispersity-effects of the precursor polymer together with the formation of mixed phases inside the SCNPs, or chemical changes of the crosslinking moieties. Traditional methods focus on analysis methods to describe their size and shape, including chromatography, microscopy, and scattering techniques. Collapsing linear precursor polymer chains into SCNPs is usually followed by size reductions that can be measured as hydrodynamic diameters d_h.[39b,72] While a non-crosslinked precursor chain is potentially able to reach its full length, the (covalently) crosslinked SCNP is normally unable to change its conformation and is trapped in its collapsed position, resulting in reduced hydrodynamic diameters compared to the precursor chain, as depicted in Fig. 2. This reduction in d_h, usually measured by gel permeation chromatography (GPC) dynamic light scattering (DLS) or diffusion-ordered NMR spectroscopy (DOSY-NMR), can be a proof of a successful single-chain collapse with solely intramolecular crosslinks and the absence of intermolecular interactions, that would lead to increased values of d_h.

Water-based GPC measurements have been used to prove the localization of hydrophobic parts of the system inside the SCNP-core.[19e,19g] After single-chain collapse, elution times should be shifted to higher retention times in SEC, indicative of lower apparent molecular weights, because of the reduced

hydrodynamic diameter of the SCNP after crosslinking. We in some cases observed an opposite trend with a shift to lower retention times or seemingly larger hydrodynamic diameters. Contrary to results from DLS and DOSY-NMR measurements, indicative of enthalpic contributions in addition to the expected entropic contribution during GPC separation.[72] This in turn hints to the formation of compartments, when comparing a precursor polymer and the resulting SCNP, as there is a significant, unexpected polarity change after the collapse reaction by hiding the non-polar parts of an amphiphilic polymer in its hydrophobic core.

Another indirect method to prove the location of the hydrophobic parts of an amphiphilic copolymer in the core of the resulting SCNPs investigates changes in the LCST behavior.[19e,19g] The cloud point temperatures T_{cp} of LCST systems are sensitive to changes of the polarity of the sample, resulting in lower T_{cp} values when hydrophobic units are contributing to the solubility of the sample. Comparing T_{cp} values of the precursor polymers to those of the resulting SCNPs shows increased T_{cp} values for the SCNPs. Hence, solubilities increase after single-chain collapses, indicating, that the hydrophobic parts of the polymers are hidden in a hydrophobic core.

Although methods like SEC, DLS, and DOSY-NMR can give good information about the hydrodynamic diameter of a SCNP and its relative change after single-chain collapse, these methods usually lack information about the SCNP's shape, since d_h is defined as the diameter of a perfect hard sphere with the same diffusion properties as the SCNP, ignoring its actual shape. Scattering techniques, such as small angle X-ray or neutron scattering (SAXS, SANS), and static light scattering (SLS), can be helpful as powerful characterization methods, providing information about the dimensions of the SCNP via its radius of gyration r_G, but additionally about its shape, e.g. if the SCNP is sparse, globular, stick-like, or compartmentalised.[20b,47a,61b,67,73]

Besides size and shape characterization in solution via chromatographic and scattering techniques, methods like atomic force microscopy (AFM) and transmission electron microscopy (TEM) have been used to visualize and analyze SCNPs in the dry state. AFM is a universal method that is theoretically able to visualize any type of SCNP. Nevertheless, its exact interpretation and comparison to other techniques like DLS or DOSY-NMR can be challenging, since the SCNPs tend to lose their shape in the dry state. This, in addition to poor resolutions with SCNP's sizes often being below the widths of the AFM cantilever tips, can lead to unreliable results.[29a,35a,74] TEM results in more accurate results for SCNPs when compared to other techniques.[59b] However, TEM is not universally applicable for all SCNPs, limited by heavy atoms required for achieving good contrasts. Although direct visualizations of the internal compartments using microscopic techniques are barely possible due to insufficient resolutions, Pomposo et al. and Meijer et al. were able to use TEM to visualize the formation of metal-based local domains inside an SCNP (see Fig. 11a);[48a,75] and high-resolution AFM to visualize differently dense parts of the SCNPs (Fig. 11b).[29a]

NMR-spectroscopy has been widely used to indirectly address compartment formations in SCNPs by analysis of
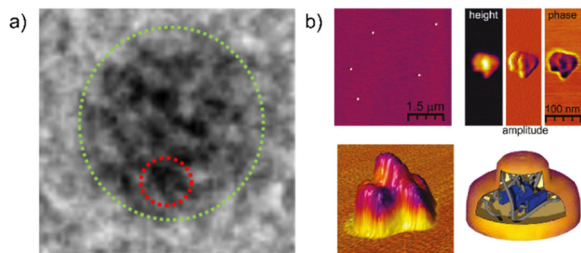
Fig. 11 (a) TEM image of local domains of a Cu-folded SCNP. Reprinted with permission from the American Chemical Society, copyright © 2018 (open access).[75] (b) High resolution AFM image of a SCNP showing a dense core and a less dense shell. Reprinted with permission from the American Chemical Society, copyright © 2010.[29a]

differences in mobility between the inner/outer parts *via* half-widths of resonances in ^{1}H-NMR spectra,[32] as a qualitative measure for the mobility of the respective chemical entities. Usually freely moving groups will show a sharp half-width, while hindered movements will result in broad signals. Hence, the chemical groups that are in the core of a compartmentalised SCNP will appear broadened in comparison to those in the less confined shell. More complex (2D)-NMR techniques, *e.g.* nuclear Overhauser effect spectroscopy (NOESY)[19b,46,62a] or T_2-relaxation[68] can give detailed information about the formation of compartments with specific chemical groups and their density inside the SCNP, in addition to STD-NMR.[76]

CW-EPR-spectroscopy on internalised radical (TEMPO) and time resolved fluorescence spectroscopy on fluorescent labels[19d,e,g] were used by us to directly reveal internal compartments inside SCNPs. Thus CW-EPR spectroscopy proved the formation of confined cores inside the SCNPs in which the TEMPO-labels were embedded, by probing spin-exchange between clustered TEMPO-molecules inside the compartment. As depicted in Fig. 12a and b Heisenberg exchange coupling had to be included in the simulations of the spectra, an effect occurring when the distance between two or more radical labels is below 1 nm, indicating high local
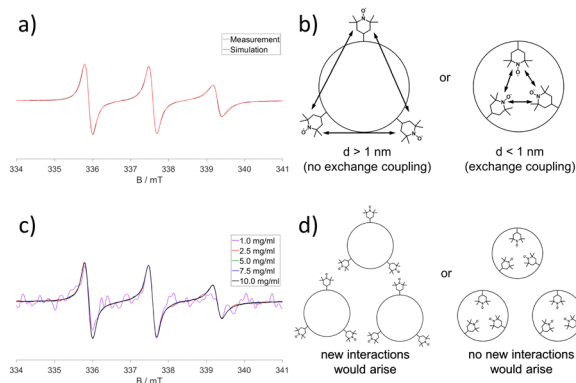

Fig. 12 CW-EPR spectroscopy of SCNPs. (a) Spectra revealed Heisenberg exchange coupling of individual TEMPO labels, included to the spectral simulation for a perfect fit. (b) Schematic interpretation of the Heisenberg exchange coupling. (c) Concentration independent shape of the spectra proving the location of the labels inside the SCNPs, and not on their surface, as depicted in (d). Reproduced and adapted with permission from Wiley VCH, copyright © 2020 (open access CC BY 4.0).[19g]
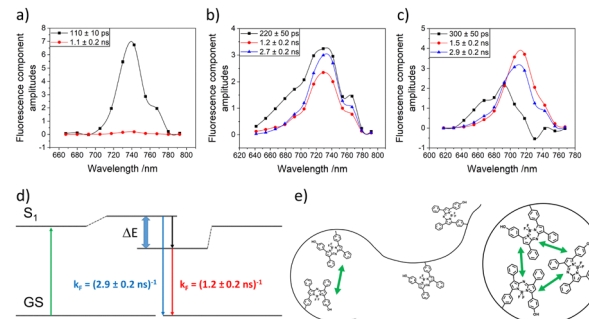

Fig. 13 Decay associated fluorescence spectra of (a) aBOD in water (KolEl), (b) the aBOD labelled linear polymer, and (c) the aBOD labelled SCNP. (d) Jablonsky diagram of the excitonic coupling of multiple aBOD molecules. (e) Schematic interpretation of the nanostructure of the aBOD labelled linear polymer and SCNP. Reproduced and adapted with permission from Wiley VCH, copyright © 2020 (open access CC BY 4.0).[19g]

concentrations of the labels. This proved the agglomeration of the labels in a confined area of the SCNP, sized smaller than 1 nm. Further concentration-dependent measurements revealed that the labels were located inside the SCNP's core, and not on its surface, as shown in Fig. 12c and d. If the labels were located in the outer shell, collisions of individual SCNPs at high concentrations would have led to at least minor changes of the shapes of the spectra, which were found to be concentration independent. (Time resolved) decay associated fluorescence spectroscopy (DAS) also represents a powerful method to understand compartmentalization in SCNPs, and was used to further confirm the results of the CW-EPR spectra by showing comparable effects, as shown in Fig. 13. Whereas a non-SCNP-bound dye (aBOD) in water fluoresced in a single exponential decay with a short fluorescence lifetime, covalently binding the same dye to a linear polymer chain created two additional decays with fluorescence lifetimes in the ns-range now embedded in polymer regions, that could form hydrophobic environments with less contact of aBOD to the fluorescence quenching water. In addition, the SCNP-bound aBOD molecules now showed the formation of excitonic couples. Similar to the Heisenberg exchange in the CW-EPR spectra, those couples only occur when two or more dye molecules are in close proximity, again proving the formation of confined structures inside the SCNPs with high local label concentrations. Other fluorescence techniques follow the formation of SCNPs and their confined structures, *via* Förster resonance energy transfer (FRET) systems inside SCNPs.[77] With this FRET system, the spatial proximity of the functionalities inside the SCNP can be proven.

5. Applications of SCNPs

Single-chain nanoparticles have various applications that arise from their extremely small size, internal and external compartments, and specific functionalities, reminiscent of catalytic sites. Thus, just like enzymes, SCNPs can be designed to act as catalysts with high catalytic activity and specificity.[16] Their enzyme-like structure is also an important factor in their application for biomedical applications.[17] Next to these two

main applications, SCNPs can also be used for detecting specific chemicals,[35b,78] antifouling,[38,61c] catching of carbon nanotubes,[57g] or as surfactants.[59a]

5.1. SCNPs as enzyme mimetic catalysts

Enzymatic reactions are usually superior in reaction speed, specificity, and activity under ambient conditions.[79] Inspired by those reactions, artificial receptors and catalysts, such as macrocyclic compounds, star or helical polymers, dendrimers, micelles, vesicles, or polymerosomes have been designed trying to copy enzymes,[16] imitating the unique internal structure of enzymes. Enzymes provide specific local environments, characterised by, e.g. hydrophobic, compartmentalised cavities which are stabilised by H-bonds, hydrophobic assemblies or disulfide bonds. Often also so-called cofactors are localised in those compartments, which additionally effect the catalytic activity. SCNPs are conceptually synthetic analoga to enzymes, based on collapsed/folded single polymer chains providing compartments with specific local properties, e.g. hydrophobic, confined environments, or the opportunity to bind catalytic sites.[15a] Meijer et al. demonstrated via CW-EPR measurements that especially the hydrophobic environment – or rather the retardation of water from those compartments – are crucial for their catalytic activity.[45d] Similar to enzymes, catalytically active SCNPs are able to provide high selectivities for reactions by providing hydrophobic compartments and confined spaces to which specific compounds can bind and react with each other, even with the possibility to bind cofactors.[47g,48a,71c,80] Both, organic as well as metal-complex catalysts can be incorporated into the hydrophobic compartments inside SCNPs that can catalyse, e.g. the reduction of ketones,[71a,73a] oxidation of alcohols,[71c] aldol reactions,[71b,71d,81] Glaser couplings,[48a,82] Sonogashira and Suzuki couplings,[47f,81,83] CuAAC,[35e,35f,80] phenol hydroxylations,[47g] photocatalytic reactions,[19a,71f,84] benzoin condensations,[47h] or intramolecular hydroaminations,[85] even in aqueous environments, in which some of those reactions are normally poor in yield or conversion. One advantage that SCNP-based, enzyme-mimetic catalytic systems have over their natural analoga is their stimuli-responsive behaviour, allowing to recycle the catalytic system while maintaining the catalytic activity.[71b,86] Biocompatibility allows their introduction into living cells, where they can perform their catalytic reactions either alone or together with natural enzymes.[35f,55g,71f] Hence, it is possible to specifically generate harmful molecules or other components inside of specific cells like tumour tissues, i.e., those cells can be killed specifically without harming healthy tissue.

5.2. SCNPs for biomedical applications

Next to their use as carriers of catalytic sites, the main field of interest in the research of compartmentalised SCNPs is in their application for biomedical purposes, providing perfect environments for the encapsulation of drugs or to covalently bind labels as imaging contrast agents. However, the design of SCNPs for biomedical applications is complex due to several basic requirements:[87] (i) water solubility; (ii) ability to carry and protect hydrophobic drugs; (iii) non-toxicity; (iv) biocompatibility/stability

in biological media; (v) biodegradability; and (vi) tissue specificity. To overcome the limitations in water solubility, the precursor polymers need to be designed to result in SCNPs with a polar shell, compatible with water. Often PEG sidechains are used to provide a proper water solubility,[43e,45f,50,61a,61b,88] e.g. using (oligo ethylene glycol) methacrylate (OEGMA) monomers as part of the precursor polymer, extended to quarternized amines,[89] alcohols,[90,91] acrylic acid,[92] or sugar carbohydrate backbones.[36a,36b,93] PEG based shells not only enable good water solubilities, but provide the SCNP with biocompatibility and low toxicity.[43e,45f,51a,61c,71f] Next to PEG, also other precursor polymer designs which are based e.g. on PNIPAM,[78b] acrylic acid,[92] or carbohydrates[36,93] can provide good biocompatibilities with cell viabilities of up to 10 mg mL^{-1}, hiding toxic entities in the cores without harming any living tissue.

Biocompatibility together with the stability of SCNPs in biological media are major issues controlling interactions within biological media, which are complex aqueous mixtures containing salts, glucose, amino acids, vitamins, and natural macromolecular assemblies like enzymes, all able to interact with, and alter the SCNP structure.[45f] Recent approaches towards biocompatible SCNPs use natural surfaces via carbohydrates, but also proteins and polypeptides have already been modified to be the basis of SCNPs with less harmful interactions with biological media.[37,94] To achieve the same biocompatibility and stability on synthetic SCNPs, the "stealth effect" can be used, mostly found for PEG based systems,[95] moving through biological media with reduced clearance.

Tissue specificity, e.g. targeting tumour tissue, can so be achieved via the enhanced permeation and retention effect.[96] This effect uses the leaky vasculature of tumours, accumulating nanoparticles only there, since the nanoparticles can easily leave the blood vessels through the leaks and enter this tissue. The chemical flexibility of SCNPs can be used to incorporate different functionalities that enable targeting of specific tissues or even specific compartments of a living cell, such as nitric oxide sensors,[78b] antigens,[36b] hormones,[92] or proteins[89] that only bind to specific tissue types. Targeting of specific cell types or cell compartments has been achieved in SCNPs by adding cell compartment specific moieties like Concanavalin A binding glucose,[93] by the formation of polyplexes,[91a] or by adjusting the surface charge of the SCNPs.[90b,91b]

6. Conclusions

Compartimentized single-chain nanoparticles (SCNPs) are novel and unique polymeric structures with a wide range of applications, especially in enzyme-mimetic catalysis and biomedical methods. There are countless possibilities to create nanosized compartments inside SCNPs for specific applications, precisely designed in view of the material (natural or synthetic), the nature of cross-linking (covalent/non-covalent/dynamic-covalent), their shape (sparse, globular, tethered), and the nature of the formed compartments. The nanosized compartments, coupled to the size of the SCNPs & their dynamics are what makes them unique candidates as catalysts, drugs, or nanooptical entities. Not only can those "subunits" be tuned via their secondary structure, the polymer

architecture, and, most prominent, the amphiphilic behaviour, but also aspects of responsivity, such as temperature-induced volume transition, be easily transferred. However, the techniques to catch the dynamic and often ambiguous nature of the internal compartments remains challenging, requiring special and combined microscopic and spectroscopic techniques, a field expanding rapidly, considering 2D-NMR-spectroscopy&EPR-methods, both probing spatially close subunits of the SCNPs, but also classical fluorescence allows to collect information about the dynamics and the binding specificity of compartments inside SCNPs. It is this detailed knowledge which pushes forward the development of SCNPs, their design and synthesis, coupled to the intricate knowledge of physics inside small confinements, as the compartments inside present.

Author contributions

Both authors have contributed to the planning, writing, and reviewing process of this article.

Data availability

All data are stored in our internal data management system and in the originally, already published papers cited in this Feature Article. Original data (all data files) are available on request, but can be collected and stored (if desired) before acceptance of the manuscript.

Conflicts of interest

There are no conflicts to declare.

Acknowledgements

Notes and references

1 L. Bar-Peled and N. Kory, *Nat. Metab.*, 2022, **4**, 1232–1244.
2 M. H. Schuler, A. M. English, T. Xiao, T. J. Campbell, J. M. Shaw and A. L. Hughes, *Mol. Cell*, 2021, **81**, 3786–3802.
3 P. Bhat, D. Honson and M. Guttman, *Nat. Rev. Mol. Cell Biol.*, 2021, **22**, 653–670.
4 J. T. Trinh, Q. Shao, J. Guan and L. Zeng, *Nat. Commun.*, 2020, **11**, 3813.
5 Y. Wu, Q. Hu, Y. Che and Z. Niu, *Chem. Sci.*, 2024, **15**, 6200–6217.
6 M.-C. Wu and T. Yow Tsong, *J. Phys. Soc. Jpn.*, 2013, **82**, 114801.
7 Y. Mai and A. Eisenberg, *Chem. Soc. Rev.*, 2012, **41**, 5969–5985.
8 J. Wang, B. Li, L. Qiu, X. Qiao and H. Yang, *J. Biol. Eng.*, 2022, **16**, 18.
9 A. V. Kabanov and S. V. Vinogradov, *Angew. Chem., Int. Ed.*, 2009, **48**, 5418–5429.
10 (a) M. Hoffmann, J. Eisermann, F. A. Schoffmann, M. Das, C. Vargas, S. Keller and D. Hinderberger, *Biochim. Biophys. Acta, Biomembr.*, 2021, **1863**, 183681; (b) M. Hoffmann, D. Haselberger, T. Hofmann, L. Muller, K. Janson, A. Meister, M. Das, C. Vargas, S. Keller, P. L. Kastritis, C. Schmidt and D. Hinderberger, *Biomacromolecules*, 2021, **22**, 3901–3912.
11 R. C. Oliver, J. Lipfert, D. A. Fox, R. H. Lo, S. Doniach and L. Columbus, *PLoS One*, 2013, **8**, e62488.
12 M. Nikzamir, Y. Hanifehpour, A. Akbarzadeh and Y. Panahi, *J. Inorg. Organomet. Polym.*, 2021, **31**, 2246–2261.
13 E. Rideau, R. Dimova, P. Schwille, F. R. Wurm and K. Landfester, *Chem. Soc. Rev.*, 2018, **47**, 8572–8610.
14 V. K. B. Adjedje, E. Schell, Y. L. Wolf, A. Laub, M. J. Weissenborn and W. H. Binder, *Green Chem.*, 2021, **23**, 9433–9438.
15 (a) E. Verde-Sesto, A. Arbe, A. J. Moreno, D. Cangialosi, A. Alegría, J. Colmenero and J. A. Pomposo, *Mater. Horiz.*, 2020, **7**, 2292–2313; (b) Y. Shao and Z. Z. Yang, *Prog. Polym. Sci.*, 2022, 133.
16 J. Rubio-Cervilla, E. Gonzalez and J. A. Pomposo, *Nanomaterials*, 2017, **7**, 341–360.
17 A. P. P. Kröger and J. M. J. Paulusse, *J. Controlled Release*, 2018, **286**, 326–347.
18 S. Wijker and A. R. A. Palmans, *ChemPlusChem*, 2023, **88**, e202300260.
19 (a) K. Mundsinger, B. T. Tuten, L. Wang, K. Neubauer, C. Kropf, M. L. O'Mara and C. Barner-Kowollik, *Angew. Chem., Int. Ed.*, 2023, **62**, e202302995; (b) K. Watanabe, N. Kaizawa, B. J. Ree, T. Yamamoto, K. Tajima, T. Isono and T. Satoh, *Angew. Chem., Int. Ed.*, 2021, **60**, 18122–18128; (c) K. Watanabe, S. Katsuhara, H. Mamiya, T. Yamamoto, K. Tajima, T. Isono and T. Satoh, *Chem. Sci.*, 2019, **10**, 3330–3339; (d) A. H. Roos, J. F. Hoffmann, W. H. Binder and D. Hinderberger, *Soft Matter*, 2021, **17**, 7032–7037; (e) J. F. Thümmler, A. H. Roos, J. Krüger, D. Hinderberger, F. J. Schmitt, G. Tang, F. G. Golmohamadi, J. Laufer and W. H. Binder, *Macromol. Rapid Commun.*, 2023, **44**, e2200618; (f) J. F. Thümmler, R. Maragani, F. J. Schmitt, G. Tang, S. M. Rahmanlou, J. Laufer, H. Lucas, K. Mäder and W. H. Binder, *Chem. Commun.*, 2023, **59**, 11373–11376; (g) J. F. Hoffmann, A. H. Roos, F. J. Schmitt, D. Hinderberger and W. H. Binder, *Angew. Chem., Int. Ed.*, 2021, **60**, 7820–7827.
20 (a) G. M. T. Huurne, A. R. A. Palmans and E. W. Meijer, *CCS Chem.*, 2019, 64–82; (b) P. J. M. Stals, M. A. J. Gillissen, T. F. E. Paffen, T. F. A. Greef, P. Lindner, E. W. Meijer, A. R. A. Palmans and I. K. Voets, *Macromolecules*, 2014, **47**, 2947–2954.
21 (a) P. H. Maag, F. Feist, V. X. Truong, H. Frisch, P. W. Roesky and C. Barner-Kowollik, *Angew. Chem., Int. Ed.*, 2023, **62**, e202309259; (b) I. Mohamed Irshadeen, V. X. Truong, H. Frisch and C. Barner-Kowollik, *Chem. Commun.*, 2022, **58**, 12975–12978.
22 N. Hosono, A. R. A. Palmans and E. W. Meijer, *Chem. Commun.*, 2014, **50**, 7990–7993.
23 D. Xiang, B. Y. Jiang, F. X. Liang, L. T. Yan and Z. Z. Yang, *Macromolecules*, 2020, **53**, 1063–1069.
24 S. Wijker, R. Monnink, L. Rijnders, L. Deng and A. R. A. Palmans, *Chem. Commun.*, 2023, **59**, 5407–5410.
25 A. E. Izuagbe, V. X. Truong, B. T. Tuten, P. W. Roesky and C. Barner-Kowollik, *Macromolecules*, 2022, **55**, 9242–9248.
26 C. K. Lyon, A. Prasher, A. M. Hanlon, B. T. Tuten, C. A. Tooley, P. G. Frank and E. B. Berda, *Polym. Chem.*, 2015, **6**, 181–197.
27 S. Mavila, O. Eivgi, I. Berkovich and N. G. Lemcoff, *Chem. Rev.*, 2016, **116**, 878–961.
28 J. A. Pomposo, I. Perez-Baena, F. Lo Verso, A. J. Moreno, A. Arbe and J. Colmenero, *ACS Macro Lett.*, 2014, **3**, 767–772.
29 (a) E. B. Berda, E. J. Foster and E. W. Meijer, *Macromolecules*, 2010, **43**, 1430–1437; (b) N. Hosono, A. M. Kushner, J. Chung, A. R. Palmans, Z. Guan and E. W. Meijer, *J. Am. Chem. Soc.*, 2015, **137**, 6880–6888; (c) F. Zhou, M. Xie and D. Chen, *Macromolecules*, 2013, **47**, 365–372; (d) N. Hosono, M. A. Gillissen, Y. Li, S. S. Sheiko, A. R. Palmans and E. W. Meijer, *J. Am. Chem. Soc.*, 2013, **135**, 501–510; (e) P. T. Dirlam, H. J. Kim, K. J. Arrington, W. J. Chung, R. Sahoo, L. J. Hill, P. J. Costanzo, P. Theato, K. Char and J. Pyun, *Polym. Chem.*, 2013, **4**, 3765–3773; (f) E. A. Appel, J. Dyson, J. del Barrio, Z. Walsh and O. A. Scherman, *Angew. Chem., Int. Ed.*, 2012, **51**, 4185–4189.
30 (a) E. Harth, B. Van Horn, V. Y. Lee, D. S. Germack, C. P. Gonzales, R. D. Miller and C. J. Hawker, *J. Am. Chem. Soc.*, 2002, **124**, 8653–8660; (b) J. Willenbacher, K. N. R. Wuest, J. O. Mueller, M. Kaupp, H. A. Wagenknecht and C. Barner-Kowollik, *ACS Macro Lett.*, 2014, **3**, 574–579; (c) S. Gillhuber, J. O. Holloway, H. Frisch, F. Feist, F. Weigend, C. Barner-Kowollik and P. W. Roesky, *Chem. Commun.*, 2023, **59**, 4672–4675.
31 (a) B. S. Murray and D. A. Fulton, *Macromolecules*, 2011, **44**, 7242–7252; (b) T. K. Claus, J. Zhang, L. Martin, M. Hartlieb, H. Mutlu, S. Perrier, G. Delaittre and C. Barner-Kowollik, *Macromol. Rapid Commun.*, 2017, 38.
32 T. Terashima, T. Sugita, K. Fukae and M. Sawamoto, *Macromolecules*, 2014, **47**, 589–600.
33 Y. Shao, Y. L. Wang, Z. Tang, Z. Wen, C. Chang, C. Wang, D. Sun, Y. Ye, D. Qiu, Y. Ke, F. Liu and Z. Yang, *Angew. Chem., Int. Ed.*, 2022, **61**, e202205183.

34 K. Watanabe, R. Tanaka, K. Takada, M. J. Kim, J. S. Lee, K. Tajima, T. Isono and T. Satoh, *Polym. Chem.*, 2016, **7**, 4782–4792.

35 (*a*) E. J. Foster, E. B. Berda and E. W. Meijer, *J. Polym. Sci., Polym. Chem.*, 2011, **49**, 118–126; (*b*) M. A. J. Gillissen, I. K. Voets, E. W. Meijer and A. R. A. Palmans, *Polym. Chem.*, 2012, **3**, 3166–3174; (*c*) B. T. Tuten, D. M. Chao, C. K. Lyon and E. B. Berda, *Polym. Chem.*, 2012, **3**, 3068–3071; (*d*) G. M. ter Huurne, M. A. J. Gillissen, A. R. A. Palmans, I. K. Voets and E. W. Meijer, *Macromolecules*, 2015, **48**, 3949–3956; (*e*) J. Chen, J. Wang, Y. Bai, K. Li, E. S. Garcia, A. L. Ferguson and S. C. Zimmerman, *J. Am. Chem. Soc.*, 2018, **140**, 13695–13702; (*f*) Y. Bai, X. Feng, H. Xing, Y. Xu, B. K. Kim, N. Baig, T. Zhou, A. A. Gewirth, Y. Lu, E. Oldfield and S. C. Zimmerman, *J. Am. Chem. Soc.*, 2016, **138**, 11077–11080; (*g*) C. H. Liu, L. D. Dugas, J. I. Bowman, T. Chidanguro, R. F. Storey and Y. C. Simon, *Polym. Chem.*, 2020, **11**, 292–297; (*h*) J. Nam, S. Kwon, Y. G. Yu, H. B. Seo, J. S. Lee, W. B. Lee, Y. Kim and M. Seo, *Macromolecules*, 2021, **54**, 8829–8838.

36 (*a*) R. Gracia, M. Marradi, U. Cossio, A. Benito, A. Perez-San Vicente, V. Gomez-Vallejo, H. J. Grande, J. Llop and I. Loinaz, *J. Mater. Chem. B*, 2017, **5**, 1143–1147; (*b*) R. Gracia, M. Marradi, G. Salerno, R. Perez-Nicado, A. Perez-San Vicente, D. Dupin, J. Rodriguez, I. Loinaz, F. Chiodo and C. Nativi, *ACS Macro Lett.*, 2018, **7**, 196–200; (*c*) N. Blanco-Cabra, J. Movellan, M. Marradi, R. Gracia, C. Salvador, D. Dupin, I. Loinaz and E. Torrents, *npj Biofilms Microbiomes*, 2022, **8**, 52.

37 (*a*) M. Hebel, J. Gacanin, T. Luckerath, D. Y. W. Ng and T. Weil, *Macromol. Rapid Commun.*, 2022, **43**, e2100413; (*b*) P. Malo de Molina, T. P. Le, A. Iturrospe, U. Gasser, A. Arbe, J. Colmenero and J. A. Pomposo, *ACS Omega*, 2022, **7**, 42163–42169.

38 X. Tian, R. Xue, F. Yang, L. Yin, S. Luan and H. Tang, *Biomacromolecules*, 2021, **22**, 4306–4315.

39 (*a*) A. Nitti, R. Carfora, G. Assanelli, M. Notari and D. Pasini, *ACS Appl. Nano Mater.*, 2022, **5**, 13985–13997; (*b*) M. K. Aiertza, I. Odriozola, G. Cabanero, H. J. Grande and I. Loinaz, *Cell. Mol. Life Sci.*, 2012, **69**, 337–346.

40 A. Sanchez-Sanchez, I. Perez-Baena and J. A. Pomposo, *Molecules*, 2013, **18**, 3339–3355.

41 A. M. Hanlon, R. W. Chen, K. J. Rodriguez, C. Willis, J. G. Dickinson, M. Cashman and E. B. Berda, *Macromolecules*, 2017, **50**, 2996–3003.

42 (*a*) O. Galant, H. B. Donmez, C. Barner-Kowollik and C. E. Diesendruck, *Angew. Chem., Int. Ed.*, 2021, **60**, 2042–2046; (*b*) O. Galant, C. E. Diesendruck and S. Spatari, *Org. Process Res. Dev.*, 2023, **28**, 1607–1617.

43 (*a*) P. J. M. Stals, M. A. J. Gillissen, R. Nicolaÿ, A. R. A. Palmans and E. W. Meijer, *Polym. Chem.*, 2013, **4**, 2584–2597; (*b*) C. C. Cheng, F. C. Chang, H. C. Yen, D. J. Lee, C. W. Chiu and Z. Xin, *ACS Macro Lett.*, 2015, **4**, 1184–1188; (*c*) J. L. Zhang, G. Gody, M. Hartlieb, S. Catrouillet, J. Moffat and S. Perrier, *Macromolecules*, 2016, **49**, 8933–8942; (*d*) H. W. van Roekel, P. J. Stals, M. A. Gillissen, P. A. Hilbers, A. J. Markvoort and T. F. de Greef, *Chem. Commun.*, 2013, **49**, 3122–3124; (*e*) C. C. Cheng, D. J. Lee, Z. S. Liao and J. J. Huang, *Polym. Chem.*, 2016, **7**, 6164–6169.

44 T. S. Fischer, D. Schulze-Sunninghausen, B. Luy, O. Altintas and C. Barner-Kowollik, *Angew. Chem., Int. Ed.*, 2016, **55**, 11276–11280.

45 (*a*) T. Mes, R. van der Weegen, A. R. Palmans and E. W. Meijer, *Angew. Chem., Int. Ed.*, 2011, **50**, 5085–5089; (*b*) M. Artar, T. Terashima, M. Sawamoto, E. W. Meijer and A. R. A. Palmans, *J. Polym. Sci., Polym. Chem.*, 2014, **52**, 12–20; (*c*) Y. Liu, T. Pauloehrl, S. I. Presolski, L. Albertazzi, A. R. Palmans and E. W. Meijer, *J. Am. Chem. Soc.*, 2015, **137**, 13096–13105; (*d*) P. J. M. Stals, C. Y. Cheng, L. van Beek, A. C. Wauters, A. R. A. Palmans, S. Han and E. W. Meijer, *Chem. Sci.*, 2016, **7**, 2011–2015; (*e*) E. Archontakis, L. Deng, P. Zijlstra, A. R. A. Palmans and L. Albertazzi, *J. Am. Chem. Soc.*, 2022, **144**, 23698–23707; (*f*) L. Deng, L. Albertazzi and A. R. A. Palmans, *Biomacromolecules*, 2022, **23**, 326–338.

46 J. Lu, N. Ten Brummelhuis and M. Weck, *Chem. Commun.*, 2014, **50**, 6225–6227.

47 (*a*) A. Sanchez-Sanchez, A. Arbe, J. Kohlbrecher, J. Colmenero and J. A. Pomposo, *Macromol. Rapid Commun.*, 2015, **36**, 1592–1597; (*b*) Z. Zhu, N. Xu, Q. Yu, L. Guo, H. Cao, X. Lu and Y. Cai, *Macromol. Rapid Commun.*, 2015, **36**, 1521–1527; (*c*) I. Berkovich, S. Mavila, O. Iliashevsky, S. Kozuch and N. G. Lemcoff, *Chem. Sci.*, 2016, **7**, 1773–1778; (*d*) F. Wang, H. Pu, M. Jin and D. Wan, *Macromol. Rapid Commun.*, 2016, **37**, 330–336; (*e*) L. N. Neumann, D. A. Urban, P. Lemal, S. Ramani, A. Petri-Fink, S. Balog, C. Weder and

S. Schrettl, *Polym. Chem.*, 2020, **11**, 586–592; (*f*) J. Willenbacher, O. Altintas, V. Trouillet, N. Knöfel, M. J. Monteiro, P. W. Roesky and C. Barner-Kowollik, *Polym. Chem.*, 2015, **6**, 4358–4365; (*g*) S. Thanneeru, S. S. Duay, L. Jin, Y. Fu, A. M. Angeles-Boza and J. He, *ACS Macro Lett.*, 2017, **6**, 652–656; (*h*) S. Garmendia, S. B. Lawrenson, M. C. Arno, R. K. O'Reilly, D. Taton and A. P. Dove, *Macromol. Rapid Commun.*, 2019, **40**, e1900071.

48 (*a*) A. Sanchez-Sanchez, A. Arbe, J. Colmenero and J. A. Pomposo, *ACS Macro Lett.*, 2014, **3**, 439–443; (*b*) H. Rothfuss, N. D. Knofel, P. W. Roesky and C. Barner-Kowollik, *J. Am. Chem. Soc.*, 2018, **140**, 5875–5881.

49 (*a*) R. K. Roy and J. F. Lutz, *J. Am. Chem. Soc.*, 2014, **136**, 12888–12891; (*b*) A. Sanchez-Sanchez and J. A. Pomposo, *J. Nanomater.*, 2015, **2015**, 1–7; (*c*) J. Liang, J. J. Struckhoff, P. D. Hamilton and N. Ravi, *Langmuir*, 2017, **33**, 7660–7668.

50 Y. Gao, V. I. Bohmer, D. Zhou, T. Zhao, W. Wang and J. M. Paulusse, *J. Controlled Release*, 2016, **244**, 375–383.

51 (*a*) E. H. H. Wong, S. J. Lam, E. Nam and G. G. Qiao, *ACS Macro Lett.*, 2014, **3**, 524–528; (*b*) E. H. H. Wong and G. G. Qiao, *Macromolecules*, 2015, **48**, 1371–1379.

52 (*a*) W. H. Binder and C. Kluger, *Curr. Org. Chem.*, 2007, **10**, 1791–1815; (*b*) W. H. Binder and R. Sachsenhofer, *Macromol. Rapid Commun.*, 2007, **28**, 15–54; (*c*) W. H. Binder and R. Sachsenhofer, *Macromol. Rapid Commun.*, 2008, **29**, 952–981; (*d*) N. Li and W. H. Binder, *J. Mater. Chem.*, 2011, **21**, 16717–16734; (*e*) D. Döhler, P. Michael and W. H. Binder, *Acc. Chem. Res.*, 2017, **50**, 2610–2620; (*f*) S. Neumann, M. Biewend, S. Rana and W. H. Binder, *Macromol. Rapid Commun.*, 2020, **41**, e1900359.

53 (*a*) M. Meldal and F. Diness, *Trends Chem.*, 2020, **2**, 569–584; (*b*) H. C. Kolb, M. G. Finn and K. B. Sharpless, *Angew. Chem., Int. Ed.*, 2001, **40**, 2004–2021.

54 M. Alqaisi, J. F. Thümmler, F. Lehmann, F.-J. Schmitt, L. Lentz, F. Rieder, D. Hinderberger and W. H. Binder, *Polym. Chem.*, 2024, **15**, 2949–2958.

55 (*a*) A. R. de Luzuriaga, N. Ormategui, H. J. Grande, I. Odriozola, J. A. Pomposo and I. Loinaz, *Macromol. Rapid Commun.*, 2008, **29**, 1156–1160; (*b*) A. R. de Luzuriaga, I. Perez-Baena, S. Montes, I. Loinaz, I. Odriozola, I. García and J. A. Pomposo, *Macromol. Symp.*, 2010, **296**, 303–310; (*c*) L. Oria, R. Aguado, J. A. Pomposo and J. Colmenero, *Adv. Mater.*, 2010, **22**, 3038–3041; (*d*) B. V. Schmidt, N. Fechler, J. Falkenhagen and J. F. Lutz, *Nat. Chem.*, 2011, **3**, 234–238; (*e*) N. Ormategui, I. García, D. Padro, G. Cabañero, H. J. Grande and I. Loinaz, *Soft Matter*, 2012, **8**, 734–740; (*f*) J. Rubio-Cervilla, H. Frisch, C. Barner-Kowollik and J. A. Pomposo, *Macromol. Rapid Commun.*, 2019, **40**, e1800491; (*g*) J. Chen, K. Li, J. S. L. Shon and S. C. Zimmerman, *J. Am. Chem. Soc.*, 2020, **142**, 4565–4569; (*h*) I. Perez-Baena, I. Loinaz, D. Padro, I. García, H. J. Grande and I. Odriozola, *J. Mater. Chem.*, 2010, **20**, 6916–6922.

56 J. F. Thümmler, R. Maragani, F.-J. Schmitt, G. Tang, S. M. Rahmanlou, J. Laufer, H. Lucas, K. Mäder and W. H. Binder, *Chem. Commun.*, 2023, **59**, 11373–11376.

57 (*a*) J. He, L. Tremblay, S. Lacelle and Y. Zhao, *Soft Matter*, 2011, **7**, 2380–2386; (*b*) W. Fan, X. Tong, Q. Yan, S. Fu and Y. Zhao, *Chem. Commun.*, 2014, **50**, 13492–13494; (*c*) P. G. Frank, B. T. Tuten, A. Prasher, D. Chao and E. B. Berda, *Macromol. Rapid Commun.*, 2014, **35**, 249–253; (*d*) C. A. Tooley, S. Pazicni and E. B. Berda, *Polym. Chem.*, 2015, **6**, 7646–7651; (*e*) W. Z. Fan, X. Tong, F. Farnia, B. Yu and Y. Zhao, *Chem. Mater.*, 2017, **29**, 5693–5701; (*f*) W. Z. Fan, X. Tong, G. Li and Y. Zhao, *Polym. Chem.*, 2017, **8**, 3523–3529; (*g*) M. Bilgi, D. K. Balta, B. A. Temel and G. Temel, *J. Polym. Sci., Polym. Chem.*, 2018, **56**, 2709–2714; (*h*) H. Frisch, J. P. Menzel, F. R. Bloesser, D. E. Marschner, K. Mundsinger and C. Barner-Kowollik, *J. Am. Chem. Soc.*, 2018, **140**, 9551–9557; (*i*) X. Ji, Y. Zhang and H. Zhao, *Chemistry*, 2018, **24**, 3005–3012; (*j*) H. Frisch, F. R. Bloesser and C. Barner-Kowollik, *Angew. Chem., Int. Ed.*, 2019, **58**, 3604–3609; (*k*) H. Frisch, D. Kodura, F. R. Bloesser, L. Michalek and C. Barner-Kowollik, *Macromol. Rapid Commun.*, 2020, **41**, e1900414.

58 C. F. Song, L. Y. Li, L. Z. Dai and S. Thayumanavan, *Polym. Chem.*, 2015, **6**, 4828–4834.

59 (*a*) F. Xu, Z. Fang, D. Yang, Y. Gao, H. Li and D. Chen, *ACS Appl. Mater. Interfaces*, 2014, **6**, 6717–6723; (*b*) J. Wen, L. Yuan, Y. Yang, L. Liu and H. Zhao, *ACS Macro Lett.*, 2013, **2**, 100–106; (*c*) W. Wen, T. Y. Huang, S. Guan, Y. B. Zhao and A. H. Chen, *Macromolecules*, 2019, **52**, 2956–2964.

60 (*a*) Z. Cui, L. Huang, Y. Ding, X. Zhu, X. Lu and Y. Cai, *ACS Macro Lett.*, 2018, **7**, 572–575; (*b*) Z. G. Cui, H. Cao, Y. Ding, P. Gao, X. H. Lu and Y. L. Cai, *Polym. Chem.*, 2017, **8**, 3755–3763.

61 (a) M. Calosi, E. Guazzelli, S. Braccini, M. Lessi, F. Bellina, G. Galli and E. Martinelli, *Polymers*, 2022, **14**, 774; (b) E. Guazzelli, E. Masotti, M. Kriechbaum, F. Uhlig, G. Galli and E. Martinelli, *Macromol. Chem. Phys.*, 2023, **224**, 2200360; (c) T. K. Nguyen, S. J. Lam, K. K. Ho, N. Kumar, G. G. Qiao, S. Egan, C. Boyer and E. H. Wong, *ACS Infect. Dis.*, 2017, **3**, 237–248.

62 (a) R. Liu and J. S. Lindsey, *ACS Macro Lett.*, 2019, **8**, 79–83; (b) R. Liu, S. J. Liu, G. F. Hu and J. S. Lindsey, *New J. Chem.*, 2020, **44**, 21293–21308; (c) S. J. Liu, J. Rong, R. Liu and J. S. Lindsey, *ACS Appl. Polym. Mater.*, 2021, **3**, 1767–1776.

63 A. Delledonne, E. Guazzelli, S. Pescina, A. Bianchera, G. Galli, E. Martinelli and C. Sissa, *ACS Appl. Nano Mater.*, 2023, **6**, 15551–15562.

64 (a) S. Wijker, L. Deng, F. Eisenreich, I. K. Voets and A. R. A. Palmans, *Macromolecules*, 2022, **55**, 6220–6230; (b) L. Deng, A. Sathyan, C. Adam, A. Unciti-Broceta, V. Sebastian and A. R. A. Palmans, *Nano Lett.*, 2024, **24**, 2242–2249; (c) L. Deng, A. R. Olea, A. Ortiz-Perez, B. Sun, J. Wang, S. Pujals, A. R. A. Palmans and L. Albertazzi, *Small Methods*, 2024, e2301072.

65 H. Zhang, L. Zhang, J. C. You, N. B. Q. Zhang, L. X. Z. Yu, H. Y. Zhao, H. J. Qian and Z. Y. Lu, *CCS Chem.*, 2021, **3**, 2143–2154.

66 X. Zhao, D. Li, J. Zhu, Y. Fan, J. Xu, X. Huang, Z. Nie and D. Chen, *ACS Macro Lett.*, 2024, **13**, 882–888.

67 S. Basasoro, M. Gonzalez-Burgos, A. J. Moreno, F. L. Verso, A. Arbe, J. Colmenero and J. A. Pomposo, *Macromol. Rapid Commun.*, 2016, **37**, 1060–1065.

68 S. Y. Liao, L. X. Wei, L. A. Abriata and F. Stellacci, *Macromolecules*, 2021, **54**, 11459–11467.

69 J. Jelken, S. H. Jung, N. Lomadze, Y. D. Gordievskaya, E. Y. Kramarenko, A. Pich and S. Santer, *Adv. Funct. Mater.*, 2022, **32**, 2107946.

70 M. A. J. Gillissen, T. Terashima, E. W. Meijer, A. R. A. Palmans and I. K. Voets, *Macromolecules*, 2013, **46**, 4120–4125.

71 (a) T. Terashima, T. Mes, T. F. De Greef, M. A. Gillissen, P. Besenius, A. R. Palmans and E. W. Meijer, *J. Am. Chem. Soc.*, 2011, **133**, 4742–4745; (b) E. Huerta, P. J. Stals, E. W. Meijer and A. R. Palmans, *Angew. Chem., Int. Ed.*, 2013, **52**, 2906–2910; (c) M. Artar, E. R. J. Souren, T. Terashima, E. W. Meijer and A. R. A. Palmans, *ACS Macro Lett.*, 2015, **4**, 1099–1103; (d) E. Huerta, B. van Genabeek, P. J. Stals, E. W. Meijer and A. R. Palmans, *Macromol. Rapid Commun.*, 2014, **35**, 1320–1325; (e) Y. L. Liu, P. Turunen, B. F. M. de Waal, K. G. Blank, A. E. Rowan, A. R. A. Palmans and E. W. Meijer, *Mol. Syst. Des. Eng.*, 2018, **3**, 609–618; (f) Y. Liu, S. Pujals, P. J. M. Stals, T. Paulohrl, S. I. Presolski, E. W. Meijer, L. Albertazzi and A. R. A. Palmans, *J. Am. Chem. Soc.*, 2018, **140**, 3423–3433.

72 J. Engelke, J. Brandt, C. Barner-Kowollik and A. Lederer, *Polym. Chem.*, 2019, **10**, 3410–3425.

73 (a) I. Perez-Baena, F. Barroso-Bujans, U. Gasser, A. Arbe, A. J. Moreno, J. Colmenero and J. A. Pomposo, *ACS Macro Lett.*, 2013, **2**, 775–779; (b) A. Sanchez-Sanchez, S. Akbari, A. Etxeberria, A. Arbe, U. Gasser, A. J. Moreno, J. Colmenero and J. A. Pomposo, *ACS Macro Lett.*, 2013, **2**, 491–495; (c) A. Sanchez-Sanchez, S. Akbari, A. J. Moreno, F. L. Verso, A. Arbe, J. Colmenero and J. A. Pomposo, *Macromol. Rapid Commun.*, 2013, **34**, 1681–1686; (d) B. Mei, A. J. Moreno and K. S. Schweizer, *ACS Nano*, 2024, **18**, 15529–15544.

74 A. P. P. Kröger, R. J. E. A. Boonen and J. M. J. Paulusse, *Polymer*, 2017, **120**, 119–128.

75 J. A. Pomposo, A. J. Moreno, A. Arbe and J. Colmenero, *ACS Omega*, 2018, **3**, 8648–8654.

76 S. Walpole, S. Monaco, R. Nepravishta and J. Angulo, *Methods Enzymol.*, 2019, **615**, 423–451.

77 P. H. Maag, F. Feist, H. Frisch, P. W. Roesky and C. Barner-Kowollik, *Chem. Sci.*, 2024, **15**, 5218–5224.

78 (a) Z. Lu, J. Zhang, W. Yin, C. Guo and M. Lang, *Macromol. Rapid Commun.*, 2022, **43**, e2200156; (b) J. Hu, M. R. Whittaker, H. Duong, Y. Li, C. Boyer and T. P. Davis, *Angew. Chem., Int. Ed.*, 2014, **53**, 7779–7784; (c) J. Pinacho-Olaciregui, E. Verde-Sesto, D. Taton and J. A. Pomposo, *Macromol. Rapid Commun.*, 2024, **45**, e2400116.

79 M. J. Wiester, P. A. Ulmann and C. A. Mirkin, *Angew. Chem.*, 2010, **123**, 118–142.

80 T. M. Xiong, E. S. Garcia, J. Chen, L. Zhu, A. J. Alzona and S. C. Zimmerman, *Chem. Commun.*, 2022, **58**, 985–988.

81 M. Meir, A. Abuaf, D. Subhomoy and M. Yithak, *RSC Adv.*, 2023, **13**, 1580–1586.

82 A. Blazquez-Martin, E. Verde-Sesto, A. Arbe and J. A. Pomposo, *Angew. Chem., Int. Ed.*, 2023, e202313502.

83 R. Lambert, A. L. Wirotius, S. Garmendia, P. Berto, J. Vignolle and D. Taton, *Polym. Chem.*, 2018, **9**, 3199–3204.

84 D. Arena, E. Verde-Sesto, I. Rivilla and J. A. Pomposo, *J. Am. Chem. Soc.*, 2024, **146**, 14397–14403.

85 P. H. Maag, F. Feist, H. Frisch, P. W. Roesky and C. Barner-Kowollik, *Macromolecules*, 2022, **55**, 9918–9924.

86 (a) S. Liu, M. Q. Tang, J. Pang, J. T. Hu, W. J. Chen, J. Cheng, Z. W. Liu, H. H. Zhao and R. Tan, *ACS Sustainable Chem. Eng.*, 2022, **10**, 11760–11772; (b) N. D. Knofel, H. Rothfuss, J. Willenbacher, C. Barner-Kowollik and P. W. Roesky, *Angew. Chem., Int. Ed.*, 2017, **56**, 4950–4954.

87 Y. Li, D. Maciel, J. Rodrigues, X. Shi and H. Tomas, *Chem. Rev.*, 2015, **115**, 8564–8608.

88 C. T. Adkins, J. N. Dobish, S. Brown and E. Harth, *ACS Macro Lett.*, 2013, **2**, 710–714.

89 J. Liu, G. Feng, R. Liu, N. Tomczak, L. Ma, G. G. Gurzadyan and B. Liu, *Small*, 2014, **10**, 3110–3118.

90 (a) A. P. P. Kroger, N. M. Hamelmann, A. Juan, S. Lindhoud and J. M. J. Paulusse, *ACS Appl. Mater. Interfaces*, 2018, **10**, 30946–30951; (b) N. M. Hamelmann, J. D. Paats and J. M. J. Paulusse, *ACS Macro Lett.*, 2021, **10**, 1443–1449.

91 (a) N. M. Hamelmann, S. Uijttewaal, S. D. Hujaya and J. M. J. Paulusse, *Biomacromolecules*, 2022, **23**, 5036–5042; (b) N. M. Hamelmann, J. D. Paats, Y. Avalos-Padilla, E. Lantero, L. Spanos, I. Siden-Kiamos, X. Fernandez-Busquets and J. M. J. Paulusse, *ACS Infect. Dis.*, 2023, **9**, 56–64.

92 A. B. Benito, M. K. Aiertza, M. Marradi, L. Gil-Iceta, T. Shekhter Zahavi, B. Szczupak, M. Jimenez-Gonzalez, T. Reese, E. Scanziani, L. Passoni, M. Matteoli, M. De Maglie, A. Orenstein, M. Oron-Herman, G. Kostenich, L. Buzhansky, E. Gazit, H. J. Grande, V. Gomez-Vallejo, J. Llop and I. Loinaz, *Biomacromolecules*, 2016, **17**, 3213–3221.

93 A. P. P. Kröger, M. I. Komil, N. M. Hamelmann, A. Juan, M. H. Stenzel and J. M. J. Paulusse, *ACS Macro Lett.*, 2019, **8**, 95–101.

94 J. E. F. Radu, L. Novak, J. F. Hartmann, N. Beheshti, A.-L. Kjøniksen, B. Nyström and J. Borbély, *Colloid Polym. Sci.*, 2007, **286**, 365–376.

95 N. J. Butcher, G. M. Mortimer and R. F. Minchin, *Nat. Nanotechnol.*, 2016, **11**, 310–311.

96 M. J. Mitchell, M. M. Billingsley, R. M. Haley, M. E. Wechsler, N. A. Peppas and R. Langer, *Nat. Rev. Drug Discovery*, 2021, **20**, 101–124.